ADVANCED MATERIALS

Supporting Information

for *Adv. Mater.*, DOI: 10.1002/adma.201702682

Dynamics of Templated Assembly of Nanoparticle Filaments within Nanochannels

*Ermanno Miele, Sanoj Raj, Zhaslan Baraissov, Petr Král, and Utkur Mirsaidov**

Supporting Information

Dynamics of Templated Assembly of Nanoparticle Filaments within Nanochannels

Ermanno Miele[1, 2, 3], *Sanoj Raj*[4], *Zhaslan Baraissov*[1, 2, 3], *Petr Král*[4,5], *and Utkur Mirsaidov*[1,2,3,6]*

1. Department of Physics, National University of Singapore, 117551, Singapore
2. Centre for BioImaging Sciences and Department of Biological Sciences, National University of Singapore, 117557, Singapore
3. Centre for Advanced 2D Materials and Graphene Research Centre, National University of Singapore, 117546, Singapore
4. Department of Chemistry, University of Illinois at Chicago, Chicago, Illinois 60607, USA
5. Department of Physics and Department of Biopharmaceutical Sciences, University of Illinois at Chicago, Chicago, Illinois 60607, USA
6. NUSNNI-NanoCore, National University of Singapore, 117411, Singapore

*Author to whom correspondence should be addressed: mirsaidov@nus.edu.sg

Table of content:

1. Wafer-scale fabrication of liquid cells with nanochannels 2
2. ζ-Potentials of the alkyl-acrylate-coated gold NPs 6
3. Atomistic molecular dynamics (MD) simulations of the NP-NP interactions 6
4. Assembly of thicker NP filaments inside the nanochannel 7
5. Assembly of NP filaments from NP chains in the nanochannel 8
6. Captions for supporting videos 9
7. Supporting references 10

1. Wafer-scale fabrication of liquid cells with nanochannels

We assembled each liquid cell from two (top and bottom) silicon (Si) chips of equal sizes (2.6 × 2.6 mm^2). Both the top and bottom chips had electron-translucent silicon nitride (SiN_x) membrane windows in the center. The lateral dimensions of the membrane windows were ~30 × 200 μm^2. The thickness of the top chip membrane was 30 nm. The thickness of the bottom chip membrane was 200 nm. The membrane of the bottom chip contained an array of 170-nm deep, 200-nm wide, and 175-μm long nanochannels with a pitch of 850 nm etched into the membrane (Figure 1A). The top chip had a 50-nm-thick Cr spacer patterned on the membrane side to keep the membranes of the top and the bottom chips of the liquid cell separated and to allow liquid between the membranes after the assembly.

We microfabricated the top and bottom chips from 200-μm-thick double-side-polished 4-inch standard (100) Si wafers. The wafers used for the fabrication of the top and the bottom chips had 30-nm and 200-nm-thick SiN_x films on both sides, respectively, and these films were deposited using low-pressure chemical vapor deposition.

Top chips: To fabricate the top chips, we first defined the central windows and grooves for cleaving the chips by patterning a SiN_x film on the wafer (opposite side of the final membranes) using conventional photolithography. Using deep reactive ion etching (DRIE) (PlasmaLab 100, Oxford Instruments, UK) of the patterned area of the SiN_x film, we exposed the underlying bulk Si on the patterned areas. Then, using a lift-off process, we patterned Cr spacers on the opposite side of the same wafer. Next, to produce the grooves and free-standing membrane windows (~30 × 200 μm^2), we etched the exposed bulk Si using a 33% (w/v) potassium hydroxide (KOH) solution at 70 °C for ~4.5 hours. During the entire microfabrication process, we protected the backside of the wafer (*i.e.*, the side with the membrane and Cr spacers), and we also ensured that the backside of the wafer did not contact the KOH solution to prevent the contamination and damage of the membrane surface and the Cr spacers. After KOH etching, we cleaved the individual chips along the patterned grooves.

Bottom chips: First, we deposited a 35-nm-thick Cr film by thermal evaporation on one side of the wafer and spin coated a positive tone e-beam resist (poly(methyl methacrylate (PMMA), A4, 950 kDa, MicroChem Corp., Newton, MA, USA) at 4000 rpm on top of the Cr film. Next, on the resist, we defined 775 sets of 197 nanochannel arrays (150-nm width lines spaced by 700 nm) on the entire wafer surface using electron beam lithography (EBL) (JEOL 6300-FS, JEOL Ltd., Tokyo, Japan). After development of the resist in a developer consisting

of methyl isobutyl ketone (MIBK) and isopropyl alcohol (IPA) (MIBK:IPA ratio of 1:3), we transferred the pattern onto the underlying Cr layer by an etch-back technique. Next, we immersed the wafer in the Cr etchant solution for 35 s (Cat.#: 651826, Sigma-Aldrich Co. LLC, St. Louis, MO, USA), which removed the exposed Cr layer and left the PMMA-protected Cr layer pattern intact. Afterward, we patterned the membranes and groves on the SiN_x film on the opposite side of the wafer in a similar manner as for the top chips described above. During this stage of membrane patterning, we ensured that each array patterned on the Cr film was aligned with the corresponding membrane. After producing the free-standing membranes and groves, we cleaved the chips from the wafer, and the final channels on free-standing SiN_x membranes were formed by removing 170 nm of the exposed SiN_x by DRIE. The DRIE parameters used for this process are given in Table S1 [1]. Along with the exposed SiN_x, the DRIE process also etched and removed PMMA on top of the Cr layer. DRIE produced nanochannels with a width of 200 nm, slightly wider than the original pattern size (width of 150 nm). Once channels were formed in SiN_x, we cleaned the chips by rinsing them first in acetone, then in IPA, and finally in deionized water, followed by gentle drying under blowing nitrogen. The Cr layer used for defining the nanochannels was etched away to expose the bare SiN_x surface with the nanochannel patterns. The detailed process flow used for fabrication of both the top and bottom chips is shown in Figure S1.

Parameters	**Cr – mask compatible**
ICP (W)	650
RF (W)	100
Gas 1 Flow CHF_3 (sccm)	30
Gas 2 Flow Ar (sccm)	0
Gas 3 Flow O_2 (sccm)	10
Gas 4 Flow N_2 (sccm)	15
Pressure (mTorr)	5
V_{bias} (V)	~30
Temperature (°C)	60

Table S1. Process parameters used in the ICP-RIE processes. A modified DRIE process was set up to achieve deep etching and acceptable roughness/uniformity using a Cr hard mask [2]. The nominal etch rate measured for the channels with defined widths of 150 nm was 2.6 nm/s.

Next, we cleaned the top and bottom chips using an oxygen plasma (RIE Vita-mini, FemtoScience, UK) with the RF power set at 150 W for 15 min. The gas flow rates for O_2 and Ar were 25 sccm and 5 sccm, respectively. Plasma cleaning was followed by a sequential acetone – IPA – deionized water cleaning process. Figure S2 displays the membrane of the bottom chip with patterned nanochannels.

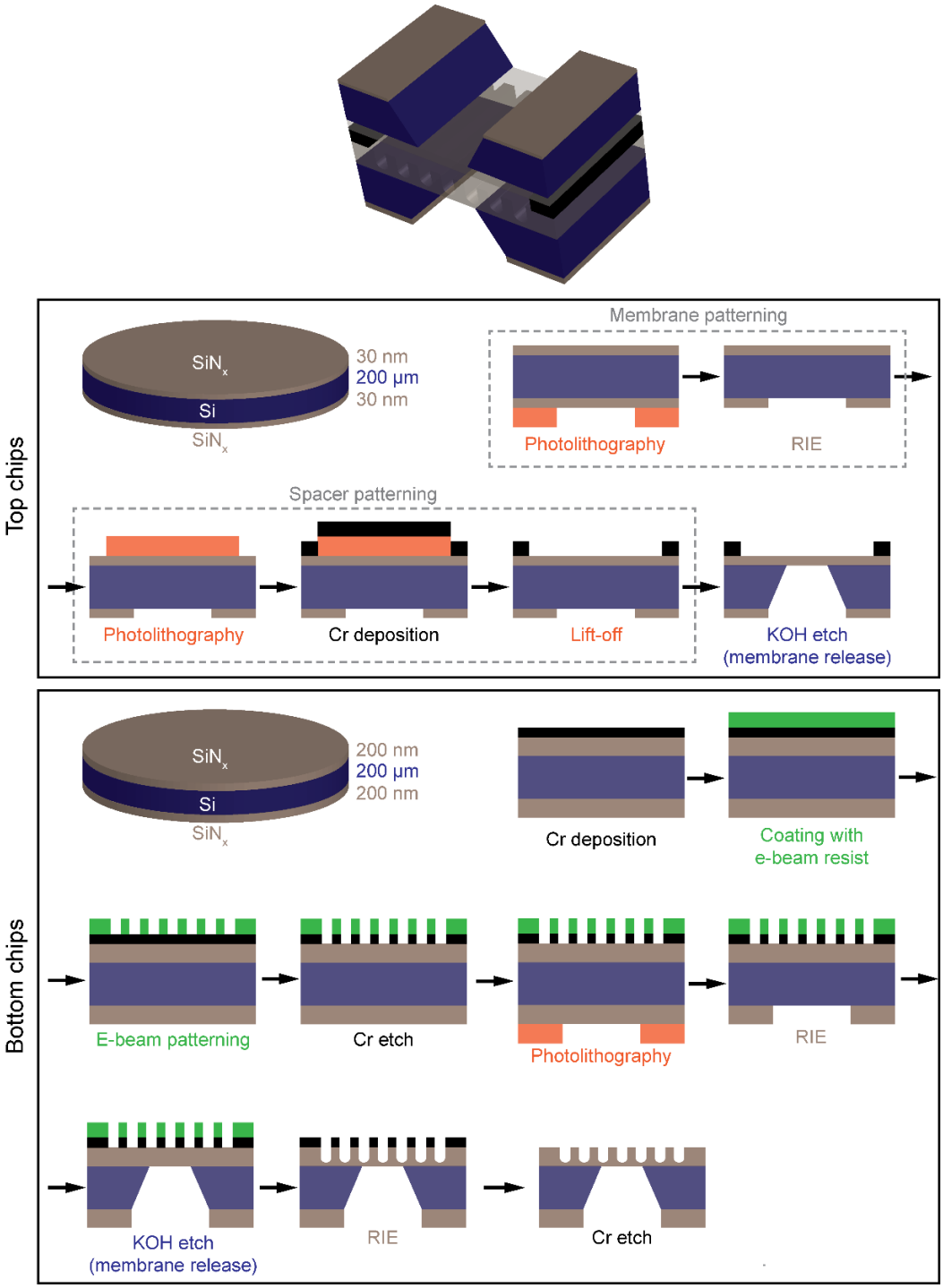

Figure S1. Process flow used for the wafer-scale fabrication of the top and bottom chips of our liquid cells for *in situ* TEM imaging. The bottom chips have membranes with nanochannels etched into them.

Before the final assembly of the liquid cells prior to each experiment, we coated the top chips with silane using vapor-phase deposition to ensure that the top membrane was hydrophobic [3]. First, we placed the clean top chips on a glass microscope slide with the membrane side of the chips facing upwards and then dispensed a few droplets of 1H,1H,2H,2H-perfluorooctyltriethoxysilane (POTS, Cat.# 667420, Sigma-Aldrich Co. LLC, St. Louis, MO, USA) on the same glass slide next to these chips. We allowed the droplets to evaporate over 30 min under vacuum in a desiccator. Next, we took the chips out of the desiccator and heated them at 120 °C for 5 min on a hotplate in a fume hood. Then, before each experiment, we plasma cleaned the SiN_x membrane side of the bottom chip and applied a solution of hydrophobic gold NPs to the membrane. Finally, we assembled the liquid cell by sealing the solution layer between the top and bottom chips with the membranes of both chips aligned to overlap for electron beam transmission.

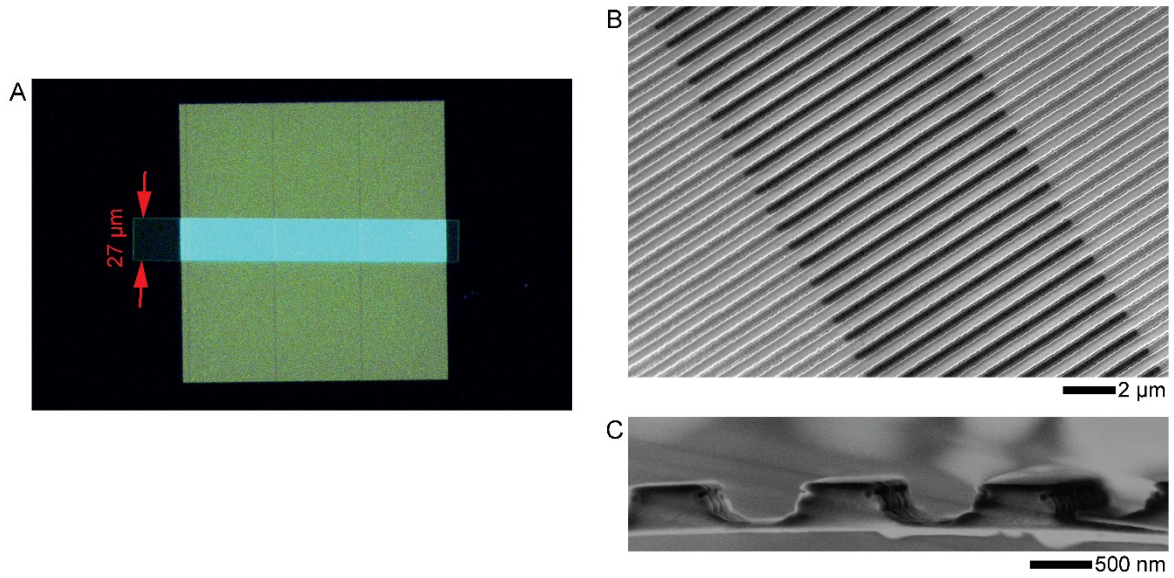

Figure S2. Patterned nanochannels on a free-standing SiN_x membrane. (**A**) Dark-field optical image of the nanochannels etched into a 200 nm-thick SiN_x film. Here, the nanochannels over the free standing SiN_x membrane and SiN_x film on top of the Si frame of the chip appear blue and green, respectively. The rectangular blue perimeter is the edge of the ~27×200 μm^2 membrane. (**B**) Scanning electron microscopy (SEM) image showing the nanochannels on the SiN_x membrane. (**C**) Cross-sectional SEM image showing the side-view profile of the nanochannels.

2. ζ-Potentials of the alkyl-acrylate-coated gold NPs

Electrostatic repulsion between the NPs in solution may affect the assembly by preventing packing and condensing of `NPs into filaments. Therefore, establishing that our NPs are effectively charge neutral is important. We measured the ζ-potential of the alkyl-acrylate-coated 10-nm NPs used in our experiments to be only approximately -10 mV (Figure S3). The small ζ-potential value is consistent with our expectations.

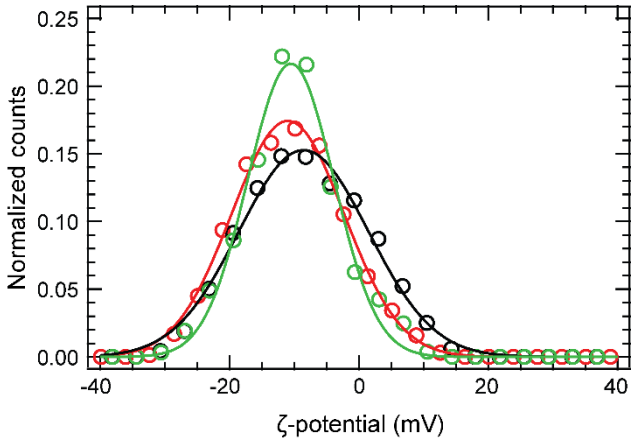

Figure S3. Measured ζ-potentials for the alkyl-acrylate-coated gold NPs used for nanofilament self-assembly. The ζ-potential values of the alkyl-acrylate-coated 10-nm NPs obtained from three measurements are centered at approximately -10 mV.

3. Atomistic molecular dynamics (MD) simulations of the NP-NP interactions

Our MD simulations revealed that ligand-ligand van der Waals (vdW) coupling between the NPs is essential for the formation of the filaments observed in our experiments. When we set the cut-off distance for the ligand-ligand vdW coupling to 1 nm, two 7.8-nm gold NPs coated with dodecyl acrylate positioned with an initial center-to-center spacing of 10.6 nm did not approach each other. The NPs approached and attached only after increasing the cut-off distance for the vdW coupling from 1 nm to 2 nm (Figure S4). At a cut-off distance of 1 nm for the ligand-ligand vdW interactions, the coated NPs only interacted via the vdW interactions of the gold cores, whereas at a cut-off distance of 2 nm, both the ligands and cores contributed to a net vdW interaction.

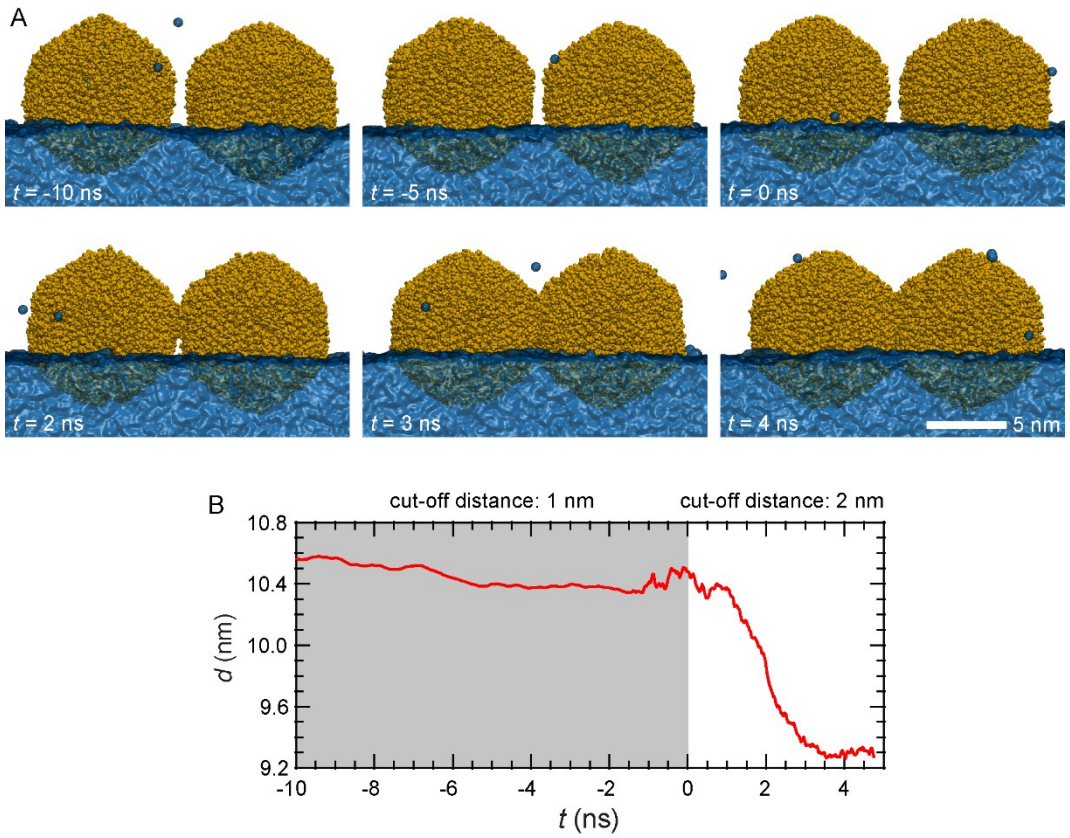

Figure S4. Interaction between two dodecyl-acrylate-coated gold NPs captured with MD simulations (Supporting Video 3). (**A**) MD simulations reveal that the attachment between two buoyant dodecyl-acrylate-coated NPs occurs through vdW interactions of their ligands. The cut-off distance for the ligand-ligand vdW coupling was set to 1 nm and 2 nm for $-\mathbf{10\ ns} < t < \mathbf{0\ ns}$ and $t > \mathbf{0\ ns}$, respectively. (**B**) Center-to-center distance between two dodecyl-acrylate-coated gold NPs obtained from the simulations shown in (A). The NPs approach each other for pairwise attachment due to the ligand-mediated vdW interactions.

4. Assembly of thicker NP filaments inside the nanochannel

When the NP density inside the nanochannel is high (≳3000 NP/μm^2), a thick NP filament forms *via* the same pathway described in the main text (Figure 2-3): buoyant NPs first aggregate in the nanochannel and then attach to form a filament (Figure S5). Next, this NP filament undergoes sideways compression to transform into a ~200-nm-wide filament with tightly packed NPs.

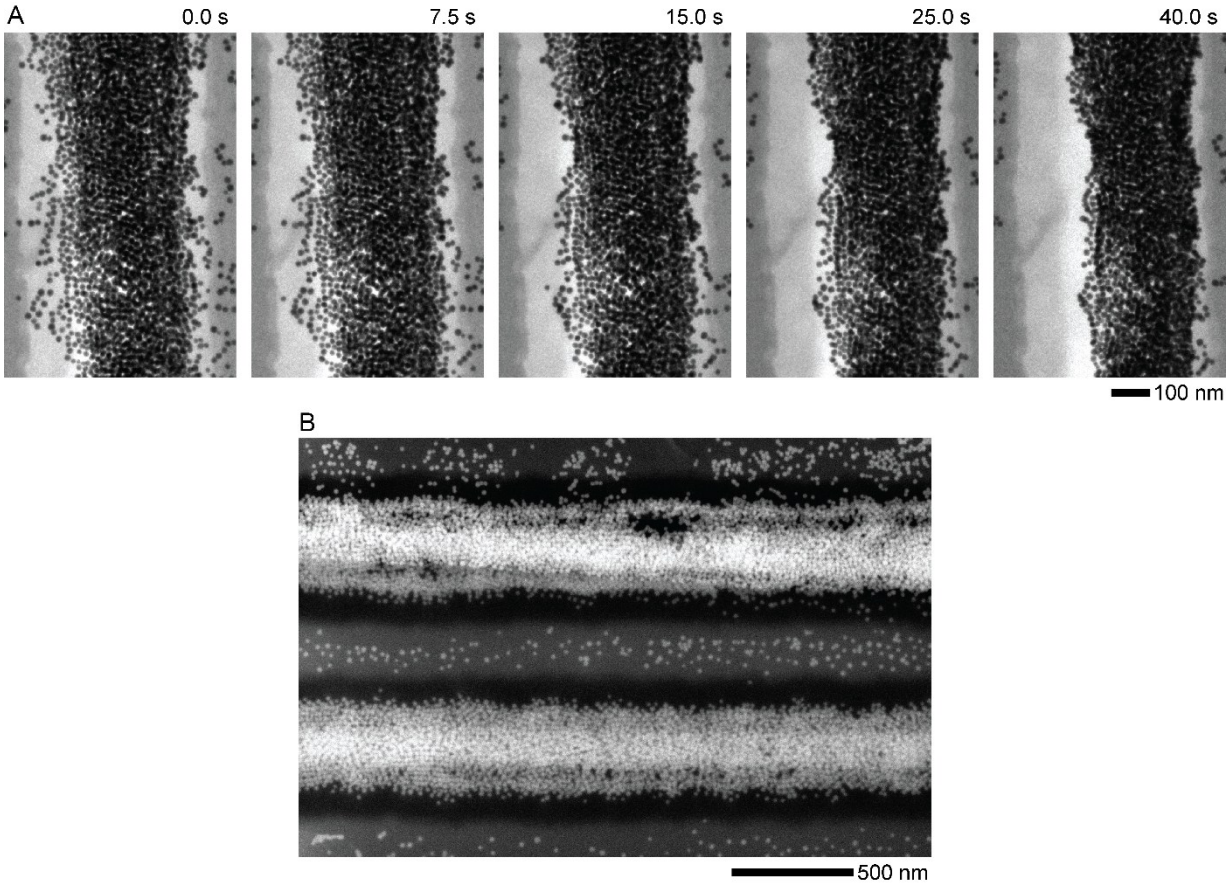

Figure S5. Formation of a NP filament in the nanochannel when the density of NPs is high. At a high NP density, the nanochannel is filled with NPs, and a filament partially pre-forms to some extent prior to TEM imaging. Only the NPs at the edge, where the NP density is low, move toward the middle of the channel before attaching to the filament (t = 0.0 s – 25.0 s). This filament consists of large number (≳3000 NP/μm^2) of NPs, and therefore, it is wider than the filaments shown in Figure 2-3.

5. Assembly of NP filaments from NP chains in the nanochannel

Under the ambient conditions, the drying of the NP suspension in the nanochannels occurs very rapidly due to the small volume of the liquid in each channel: ($V_{channel} \approx 0.5(\pi R^2 L) = 0.5(\pi \times (200\ \text{nm})^2 \times 175.6\ \mu\text{m}) \approx 11.0\ \text{fL}, R \approx 200$ nm, $L \approx 175.6$ μm (or 630 aL in the field of view, $L_{\text{field of view}} \approx 10\ \mu m$). Our observations showed that filament formation occurs on the time scale > 1 min. Therefore, because of this rapid drying process under ambient conditions, we expect the NPs to only settle at the bottom of the nanochannel without having sufficient time to form filaments. To explore if the wetting of the nanochannel containing these settled NPs forces filament formation, we imaged dry nanochannels with settled NPs. Figure S6A shows that, as the liquid flows into the nanochannel (contrast darkens inside the nanochannel), the NPs detach from the bottom of the channel and slowly

(~70 s) move toward each other condensing into a filament in the center of the channel. The presence of the liquid inside the nanochannel enables the filament formation by providing sufficient time for NP assembly. In the absence of the liquid, the NPs remain at the bottom of the channel and do not assemble into a filament (Figure S6B).

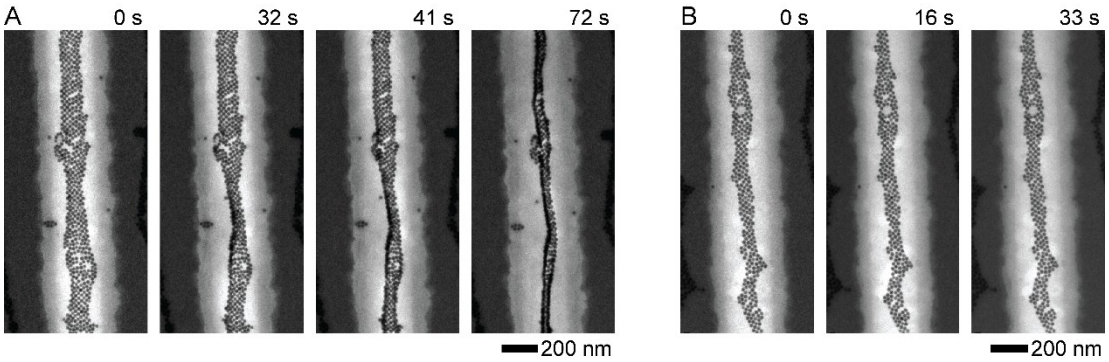

Figure S6. Driving the assembly of dry NPs into a NP filament inside the nanochannel during wetting. (**A**) Dry NPs at the bottom of the nanochannel (t = 0 s) slowly condense into a NP filament when the nanochannel starts to wet (t = 72 s). The darkening contrast of the nanochannel is indicative of the nanochannel wetting. (**B**) In the absence of the fluid, the dry NPs at the bottom of the nanochannel remain intact and do not form a filament.

6. Captions for supporting videos

Supporting Video 1: Assembly dynamics of the NPs into a thin filament inside the nanochannel. The initial density of the NPs in the nanochannel is ~200 NP/μm^2.

Supporting Video 2: Assembly dynamics of the NPs into a thicker and rigid filament inside the nanochannel. The initial density of the NPs in the nanochannel is ~1100 NP/μm^2.

Supporting Video 3: MD simulation showing the interaction between two dodecyl-acrylate-coated gold NPs. Here, the cut-off distance for the ligand-ligand vdW coupling was set to 1 nm and 2 nm for $-10\ \text{ns} < t < 0\ \text{ns}$ and $t > 0$ ns, respectively.

Supporting Video 4: Fragmentation dynamics of the NP filament during the filament assembly process. Fragmentation occurs when two NP-dense regions fail to connect due to a low local density of NPs.

7. Supporting references

[1] C. Reyes-Betanzo, S. A. Moshkalyov, M. A. Cotta, M. A. Pavanello, A. C. S. Ramos, J. W. Swart, J. Vacuum Sci. Technol. A 1999, 17, 3179.
[2] T. C. Mele, Journal of Vacuum Science & Technology B: Microelectronics and Nanometer Structures 1984, 2, 684.
[3] A. Tuteja, W. Choi, M. Ma, J. M. Mabry, S. A. Mazzella, G. C. Rutledge, G. H. McKinley, R. E. Cohen, Science 2007, 318, 1618.